

Magnetohydrodynamic Free Convective Boundary Layer Flow of a Nanofluid past an Impulsively Started Flat Vertical Plate with Newtonian Heating Boundary Condition

¹Stephenson Mandere Magoma, ²Prof. Johanah Sigey,
³Dr. Jeconia Abonyo Okelo, ⁴Dr. James Mariita Okwoyo,

¹ (Msc. student) Department of Pure and Applied Mathematics, Jomo Kenyatta University of Agriculture and Technology, Nairobi, KENYA,

²Department of Pure and Applied Mathematics, Jomo Kenyatta University of Agriculture and Technology, Nairobi, KENYA,

³Department of Pure and Applied Mathematics, Jomo Kenyatta University of Agriculture and Technology, Nairobi, KENYA,

⁴School of Mathematics, University of Nairobi, Nairobi, KENYA,

Abstract: Steady two dimensional MHD free convective boundary layer flow of an electrically conducting Newtonian nanofluid past an impulsively started infinite vertical plate is investigated numerically. Nanofluids are well-dispersed (metallic) nanoparticles at low-volume fractions in liquids. They may enhance the mixture's properties among them, thermal conductivity over the base fluid values. A magnetic field can be used to control the motion of an electrically conducting fluid in micro-scale systems used for the transportation of fluids. The momentum and energy equations along with the boundary conditions are first converted into dimensionless form by dimensional analysis. The transformed equations are solved numerically using the Implicit Finite Difference method of order two. MATLAB software is used to obtain the solutions of the tri-diagonal matrices. The effects of different controlling parameters, namely; Prandtl number, magnetic field number, Grashof number and Eckert number on temperature and velocity profiles are investigated. The numerical results for the velocity and temperature profiles are discussed and presented on tables and graphs. It is found that the fluid velocity increases with increase in the magnetic field and the Grashof number as temperature values also increase with increase of Prandtl number and Eckert number.

Key words: Magnetohydrodynamics, Laminar, Newtonian heating, Boundary layer, Nanofluid.

I. Introduction

A nanofluid is a dilute suspension of nanometer-sized particles and fibres dispersed in a liquid. Accordingly, their physical properties such as; velocity, density, thermal and electrical conductivities are superior as compared with those of the base fluids. The most important of the physical properties of nanofluids, is thermal conductivity owing to its many applications.

The conventional fluids such as water, oil and ethylene glycol mixtures exhibit poor thermal conductivity and therefore are not very suitable for heat transfer. Their application as cooling tools can increase manufacturing and operating costs. To enhance the thermal conductivity of these fluids, nanoparticles are suspended in these liquids. Nanofluids are made of ultrafine nanoparticles of the order of <100nm suspended in a base fluid such as water or an organic solvent. Nanofluids are found to exhibit higher conductive, minimum clogging, boiling and convective heat transfer performances as compared to the conventional fluids as was observed by Alkharinia et al (2011).

Nanotechnology has many potential applications such as in agriculture, pharmaceutical and biological sensors. Potential forms of nanomaterials available for use in biotechnological applications include nanowires, nanofibres, nanomachines and nanostructures. Engineering applications for development of biomedical devices and procedures, an investigation by Kuznetsov and Hobson (2011). Industrial applications of nanofluids include electronics, automotives and nuclear energy. Despite significant progress on nanofluids, experimental findings have been relatively inconsistent at times controversial and present theories do not fully explain the mechanisms of the elevated thermal conductivity and convection heat transfer performance. This was observed by Keblinski et al (2008).

MHD is the branch of science that studies the behavior of an electrically conducting fluid such as plasma or molten metal acted on by a magnetic field. It is the study of dynamics of electrically conducting fluids. The fundamental concept behind MHD is that Magnetic fields can induce currents in a moving conductive fluid which in turn generate forces on the fluid and the induced electric current changes the magnetic

field. The application of the magnetic field produces Lorentz forces which are able to transport liquid in the mixing processes as an active micro mixing technology method.

MHD flow past a flat surface has many important technological and industrial applications such as micro MHD pumps, micro mixing of physiological samples and drug delivery as observed by Carpretto et al (2011).

Transportation of conductive biological fluid in Microsystems may greatly benefit from the theoretical research in this area Yazdi et al (2011).

Newtonian heating is a situation where the heat is transported to a convective fluid via a bounding surface having finite heat capacity. These situations arise in several important engineering devices namely; heat exchanger where the conduction in the solid tube wall is influenced by the convection in the fluid past it Merkin et al (2012) and the conjugate heat transfer around fins where the conduction within the fin and the convection surrounding the fin must be analyzed simultaneously to obtain important design information.

II. Objectives Of The Study

2.1. General objectives

To study MHD free convective boundary layer flow of a nanofluid past a flat vertical plate with Newtonian heating boundary condition.

2.1.1. Specific research objectives

- i). To investigate the effect of the rate of heat and mass transfer on Newtonian heating parameter.
- ii). To determine axial velocity.
- iii). To determine fluid temperature

III. Literature Review

Studies on MHD free convective boundary-layer flow of nanofluids are very limited. Recent studies carried out by Chamkha and Aly (2011) on MHD free convective boundary-layer flow of a nanofluid along a permeable isothermal vertical plate in the presence of heat source or sink which presented non-linear solutions. Nourazar et al (2011) examined MHD forced convective flow of nanofluid over a horizontal stretching flat plate with variable magnetic field including the viscous dissipation. In addition, Zeesham et al (2012) investigated the MHD flow of third grade nanofluid between coaxial porous cylinders while Martin et al (2012) investigated MHD mixed convective flow of nanofluid over a stretching sheet.

Natural convective flow of a nanofluid past a vertical plate under different boundary conditions has been investigated by several researchers. Ho et al (2008) studied natural convection flow of a nanofluid under various flow configurations. Niu et al (2012) investigated slip-flow and heat transfer of a non-Newtonian nanofluid in a microtube. Kuznetsov and Nield (2010) studied natural convective flow of a nanofluid past a vertical plate, Khan and Aziz (2011) used Buongiorno (2006) model to investigate boundary layer flow of a nanofluid past a vertical surface with a constant heat flux.

From the above cited research analysis of the free convective boundary layer flow of a nanofluid past a flat vertical plate with Newtonian heating boundary condition requires more investigation owing to the numerous applications as has been aforementioned, and this forms the basis of this study.

IV. Geometry Of The Problem

The current problem is that of two-dimensional steady laminar free convective boundary layer flow over a permeable flat vertical plate. The flow configuration and coordinate system below presents the geometry.

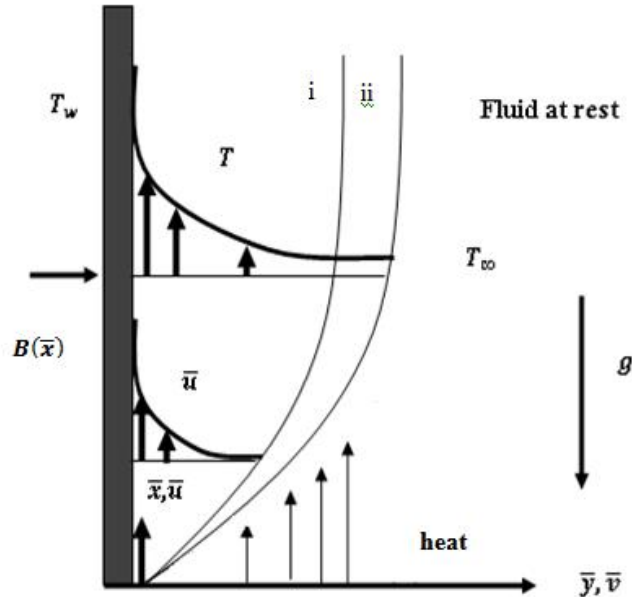


Figure 1. Flow configuration and coordinate system

Figures i,ii, above represent momentum and thermal boundary layers.

It is assumed that the surface of the plate is subject to Newtonian boundary heating condition (NH).

A transverse magnetic field with variable strength $\mathbf{B}(\bar{x})$ is applied parallel to the \bar{y} axis.

It is assumed that the magnetic Reynolds number is small and hence the induced magnetic field can be neglected. The tangential and normal velocities of the fluid are respectively taken as \bar{u} and \bar{v} . The fluid temperature is denoted by T . the Oberbeck – Boussinaq approximation is used.

4.1 Governing Equations

Various equations governing the flow problem will be derived, non-dimensionalized and solved using the Implicit Finite Difference method of order two. In order to describe the phenomenon mathematically the following assumptions are made;

1. The magnetic Reynolds number is small and therefore the induced magnetic field can be neglected.
2. The surface of the plate is subject to Newtonian heating boundary condition.

In the MHD problem, conservation equations are solved. They include the conservation of mass, conservation of momentum and conservation of energy.

4.1.1 Equation of continuity

This is derived from the law of conservation of mass which states that mass can neither be created nor destroyed and is expressed as;

$$\frac{\partial \rho}{\partial t} + \nabla \cdot (\rho \mathbf{v}) = 0 \quad (1)$$

4.1.2 Momentum equation

This is derived from Newton's second law of motion which states that the sum of resultant forces equal to the rate of change of momentum of the flow.

Momentum equation in tensor form is given by:

$$\frac{\partial u_i}{\partial t} + u_j \frac{\partial u_i}{\partial x_j} = -\frac{1}{\rho} \frac{\partial p_i}{\partial x_i} + \nu \nabla^2 u_i + F_i \quad (2)$$

4.1.3 The Lorentz force term

This is the entire electromagnetic force on a charged particle q , given by;

$\mathbf{F} = q\mathbf{E} + q\mathbf{v} \times \mathbf{B}$ where q is the charged particle, \mathbf{E} is the electric field by divergence it can be given as;

$$\mathbf{F} = \frac{(\mathbf{B} \cdot \nabla) \mathbf{B}}{\mu_0} - \nabla \left(\frac{B^2}{2\mu_0} \right) \quad (3)$$

Where the first term on the right is magnetic tension force and the second term is the magnetic pressure force.

4.1.4 Ideal Ohm's law for plasma

Neglecting Hall current, pressure gradient, inertial and resistive terms, it can be expressed as:

$$E + \nabla \times B = 0 \tag{4}$$

4.1.5 Energy equation

This is derived from the first law of thermodynamics which is the law of conservation of energy and states that the energy of an isolated system is constant; energy cannot be created nor destroyed but can be transformed from one form to another.

In tensor form it is given by;

$$\rho c_v \left(\frac{\partial Q}{\partial t} + U_i \frac{\partial Q}{\partial x_i} \right) = \frac{\partial}{\partial x_i} \left(K \frac{\partial Q}{\partial x_i} \right) + \mu \left(\frac{\partial u_i}{\partial x_i} + \frac{\partial u_i}{\partial x_i} \right)^2 \tag{5}$$

4.2 Dimensional Analysis

The dimension of any physical quantity is the combination of the basic physical dimensions that compose it. Some fundamental physical dimensions are length, mass, time and electrical charge. All other physical quantities can be expressed in terms of these fundamental dimensions. Dimensional analysis therefore checks relations among physical quantities by identifying their dimensions.

It reduces complex physical problems to simpler forms to give a quantitative answer. Bridgman (1969) explains it as: “the principal use of dimensional analysis is to deduce from a study of the dimensions of the variables in any physical system, certain limitations on the form of any possible relationship between those variables. The method is of great generality and mathematical simplicity”. In this study, dimensional analysis has been used in the non-dimensionalization of the governing equations by first selecting certain characteristic quantities and then substituting them in the equations.

4.2.1 Finite Difference Method

Implicit FD method of order two has been used to solve the PDE and involves the following steps:

- (i). Generate a grid, for example (x_i, t_k) , where we want to find an approximate solution.
- (ii). Substitute the derivatives in the PDEs with finite difference schemes. The PDEs then become linear algebraic equations.
- (iii). Solve the algebraic equations.

In a finite difference grid to calculate the values at the mesh points, each nodal point is identified by a double index (i, j) that defines its location with respect to t and x as indicated below:

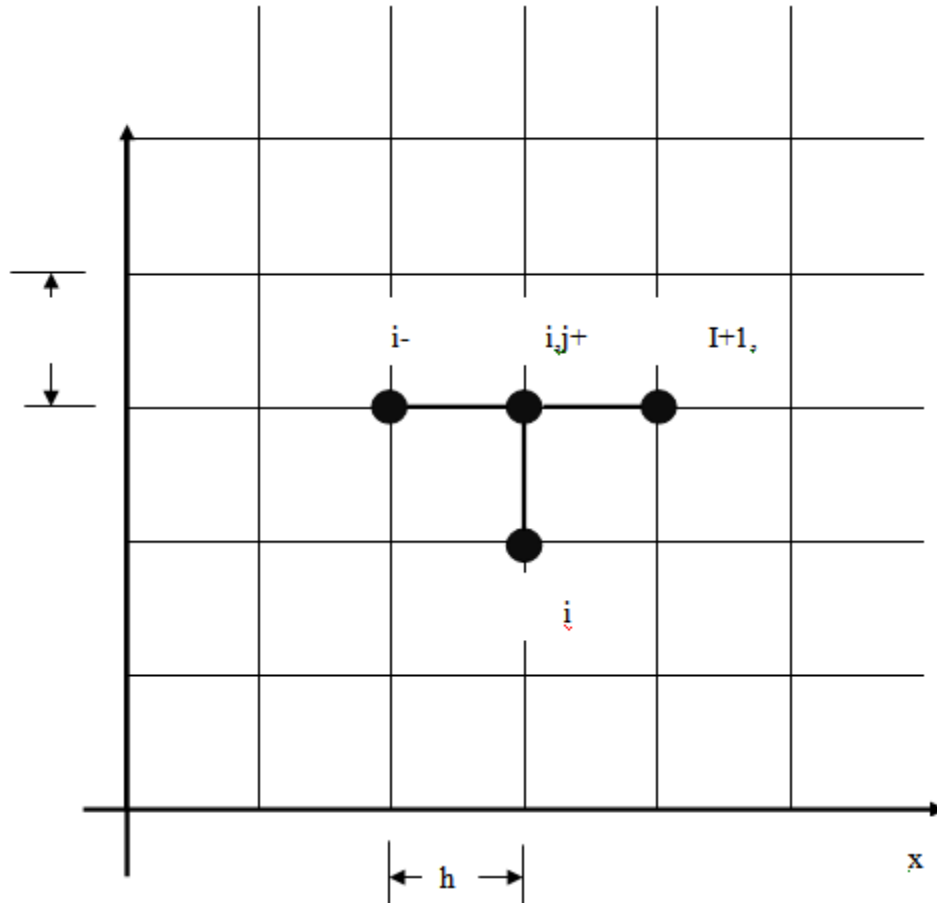


Figure 2. Grid points

If we use the backward difference at time t_{j+1} and a second-order central difference for the space derivative at position x_i (The Backward Time, Centered Space Method “BTCS”) we get the recurrence equation:

$$\frac{u_{i,j+1} - u_{i,j}}{k} = \frac{u_{i+1,j+1} - 2u_{i,j+1} + u_{i-1,j+1}}{h^2}$$

We obtain $u_{i,j+1}$ from solving the linear equations:

$$(1 + 2r)u_{i,j+1} - ru_{i-1,j+1} - ru_{i+1,j+1} = u_{i,j}$$

where $r = k/h^2$ and $\frac{\partial u}{\partial t} = \left(\frac{u_{i-1,j+1} - 2u_{i,j+1} + u_{i+1,j+1}}{h^2} \right)$

The scheme is always numerically stable and convergent.

4.2.2 Methodology

In this study we have developed Implicit Crank Nicholson numerical scheme and used finite difference method to solve the momentum and energy equations. The method obtains a finite system of linear or nonlinear algebraic equations from the PDE by discretizing the given PDE and coming up with the numerical schemes analogues to the equation, in our case the momentum and energy equations. We have solved the equations subject to the given boundary conditions. Math lap software was used to generate solution values in this study.

4.2.3 Discretisation Of Partial Derivatives

The finite difference technique basically involves replacing the partial derivatives occurring in the partial differential equation as well as in the boundary and initial conditions by their corresponding finite difference approximations and then solving the resulting linear algebraic system of equations by a direct method or a standard iterative procedure. The numerical values of the dependent variable are obtained at the points of intersection of the parallel lines, called mesh points or nodal point.

4.3 Mathematical Formulation

Consider a two dimensional steady laminar free convective boundary layer flow of a nanofluid over a permeable flat vertical plate as shown in **Fig. 1** (i), (ii) represent momentum and thermal boundary layers). The

ambient value of the temperature is denoted by T_∞ . It is assumed that the surface of the plate is subject to Newtonian heating boundary condition (NH). A transverse magnetic field with variable strength $B(\bar{x})$ is applied parallel to the \bar{y} axis. It is assumed that the magnetic Reynolds number is small and hence the induced magnetic field can be neglected. The tangential and normal velocities of the fluid are respectively taken as \bar{u} and \bar{v} . The fluid temperature is denoted by T . The Oberbeck–Boussinesq approximation is used. With these assumptions and the standard boundary layer assumptions, the governing equations can be written as (Aziz A, Khan WA (2012))

$$\frac{\partial p}{\partial x} = \mu \frac{\partial^2 \bar{u}}{\partial \bar{y}^2} - \rho_f \left(\bar{u} \frac{\partial \bar{u}}{\partial y} + \bar{v} \frac{\partial \bar{u}}{\partial y} \right) \tag{6}$$

$$+ \left[(1 - C_\infty) \rho_{f\infty} g (T - T_\infty) - (\rho_f - \rho_{f\infty}) g (C - C_\infty) \right] - \sigma_o B^2(\bar{x}) \bar{u}^2$$

$$\bar{u} \frac{\partial T}{\partial y} + \bar{v} \frac{\partial T}{\partial y} = \alpha \frac{\partial^2 T}{\partial y^2} + \tau \left[\frac{\partial C}{\partial y} \frac{\partial T}{\partial y} + \frac{1}{T_\infty} \left(\frac{\partial T}{\partial y} \right)^2 \right] \tag{7}$$

subject to the boundary conditions(Narahari M, Dutta BK (2012))

$$\bar{u} = 0 \text{ at } \bar{y} = 0$$

$$\bar{u} \rightarrow 0 \quad T \rightarrow T_\infty \text{ as } \bar{y} \rightarrow \infty \tag{8}$$

where $\tau = \frac{(\rho c)_p}{(\rho c)_f}$ is the ratio of nanoparticle heat capacity and the base fluid heat capacity, $\alpha = \frac{k}{(\rho c)_f}$ is the

thermal diffusivity of the fluid, ρ_f is the density of the base fluid, μ, k are viscosity, thermal conductivity of the base fluid and ρ_p is the density of the particles, g is the acceleration due to gravity, $\sigma = \sigma_o \bar{u}$ is the

variable electric conductivity σ_o is the constant electric conductivity, $B(\bar{x}) = \frac{B_o^2}{\bar{x}^{\frac{1}{2}}}$ is the variable magnetic

field, B_o is the constant magnetic field. \bar{x} -axis is taken along the plate in the vertical upward direction, \bar{y} -axis is taken normal to the plate in the direction of the applied magnetic field, \bar{u} is the velocity component in the x-directions and \bar{t} is dimensional time.

4.3.1 Nondimensionalization

Consider the steady free convective flow of a radiating viscous incompressible and electrical conducting nanofluid past an impulsively started infinite vertical plate with Newtonian heating.

The x -axis is taken along the plate in the vertical upward direction and the y -axis is normal to the plate in the direction of the applied magnetic field. Initially, the plate and the fluid assumed the same temperature T_∞ at the time $t \leq 0$. At time $t > 0$, the plate is given an impulsive motion in the vertical upward direction against gravitational field with a velocity U_o . The rate of heat transfer from the surface is assumed to vary directly to the local surface temperature T. As the plate is considered infinite in x -direction, all the physical variables are function of y and t only. Then, the fully developed flow of a gas is governed by the following set of equations under the usual Boussinesq's approximation:

$$\frac{\partial u}{\partial t} = \nu \frac{\partial^2 u}{\partial y^2} + g \beta (T - T_\infty) - \frac{\sigma \beta_o^2 U}{\rho} \tag{9}$$

$$\rho C_p \frac{\partial T}{\partial t} = \kappa \frac{\partial^2 T}{\partial y^2} + \mu \left(\frac{\partial u}{\partial y} \right)^2 \tag{10}$$

with the following initial and boundary conditions

$$U = 0, T = T_\infty \text{ for all } y. \quad t > 0 \quad U = U_0 \text{ at } y = 0 \tag{11}$$

where U is a velocity component in x -directions, ρ is the density, g is the acceleration due to gravity, T is the temperature of the fluid, C_p is the specific heat at constant pressure, β is the coefficient of thermal expansion, κ is the thermal conductivity and σ is the electrical conductivity, ν is the kinematic viscosity, μ is the viscosity of the fluid, B_0 is the strength of the magnetic field. The equation of continuity is identically satisfied.

In the optically thin limit, the fluid does not absorb its own emitted radiation which implies that there is no self-absorption but rather the fluid absorbs radiation emitted by the boundaries. Introducing the following dimensionless quantities;

$$U = \frac{\bar{U}}{U_0}, t = \frac{\bar{t} \bar{U}^2}{\nu}, y = \frac{\bar{y} \bar{U}}{\nu} \tag{12}$$

Equations (3.1) and (3.2) respectively become

$$\frac{\partial u}{\partial t} = \frac{\partial^2 u}{\partial y^2} + G\theta + \tau [g\beta(T - T_\infty)] - \sigma_0 M^2 U \tag{13}$$

$$\frac{\partial \theta}{\partial t} = \frac{1}{Pr} \frac{\partial^2 \theta}{\partial y^2} + \tau \left[\frac{\partial \theta}{\partial y} + E_c \left(\frac{\partial U}{\partial y} \right)^2 \right] \tag{14}$$

Where $\tau = \frac{(\rho c)_p}{(\rho c)_f}$ is the ratio of nanoparticle heat capacity and the base fluid heat capacity, $Pr = \frac{C_p \mu}{\kappa}$ is

prandtl number, $M = \frac{\nu \sigma B_0^2}{\rho U_0^2}$ is the magnetic field parameter, $E_c = \frac{U_0^2}{C_p T_\infty}$ is the Eckert number,

$$G = \frac{\nu g \beta T_\infty}{U_0^3} \text{ is the Grashof number and } \theta = \frac{T - T_\infty}{T_\infty}$$

The initial and boundary conditions (8) in dimensionless forms becomes

$$t \leq 0, U = 0, \theta = 0, y = 0 \quad t > 0, U = 1, \theta = 1, \text{ for all } y \tag{15}$$

4.3.2 Numerical Technique

To solve the unsteady non-linear coupled partial differential equations (13) and (14) under the initial and boundary conditions (15), an implicit finite difference method of Crank Nicolson type is used. The finite difference equations corresponding to equations (13) and (14) are discretized using Nicolson method as follows:

$$\frac{U_{i,j+1} - U_{i,j}}{\Delta t} = \frac{1}{2} \left[\frac{U_{i+1,j+1} - 2U_{i,j+1} + U_{i-1,j+1} + U_{i-1,j} - 2U_{i,j} + U_{i+1,j}}{(\Delta t)^2} \right] \tag{16}$$

$$+ M \left[\frac{U_{i,j+1} - U_{i,j}}{2} \right] + G \left[\frac{\theta_{i,j+1} + \theta_{i,j}}{2} \right]$$

$$\frac{\theta_{i,j+1} - \theta_{i,j}}{\Delta t} = \frac{1}{Pr} \left[\frac{\theta_{i,j+1} - 2\theta_{i,j} + \theta_{i,j-1}}{(\Delta y)^2} \right] + E_c \left[\frac{U_{i,j+1} - U_{i,j}}{\Delta t} \right]^2 \tag{17}$$

4.4 Results And Discussion

4.4.1 Momentum Equation

The equation

$$\frac{\partial u}{\partial t} = \frac{\partial^2 u}{\partial y^2} + G\theta + \tau [g\beta(T - T_\infty)] - \sigma_0 M^2 U \tag{18}$$

Where M and G are the magnetic field and Grashof numbers respectively. The equation is solved subject to the boundary conditions $U_{i,0} = 0$ and $\theta_{i,0} = 0$ for all i except i=0, and

$$U_{0,n+1} = U_{2,n+1} = 0 \quad U_{0,n+1} = 0 \tag{19}$$

4.4.2 Implicit Crank Nicholson Numerical Scheme

We develop Implicit Crank Nicholson numerical scheme and discretize equation (18) as follows;

$$\frac{U_{i,j+1} - U_{i,j}}{\Delta t} = \frac{1}{2} \left[\frac{U_{i+1,j+1} - 2U_{i,j+1} + U_{i-1,j+1} + U_{i-1,j} - 2U_{i,j} + U_{i+1,j}}{(\Delta t)^2} \right] + M \left[\frac{U_{i,j+1} - U_{i,j}}{2} \right] + G \left[\frac{\theta_{i,j+1} + \theta_{i,j}}{2} \right] \tag{20}$$

$\Delta t = \Delta y = 0.05$

Taking i=1, j=1, 2, 3.....our y=i and t=j, M=0.1 and G=2, we get the matrix equation

$$\begin{bmatrix} 2.9975 & -1 & 0 & 0 & 0 & 0 \\ -1 & 2.9975 & -1 & 0 & 0 & 0 \\ 0 & -1 & 2.9975 & -1 & 0 & 0 \\ 0 & 0 & -1 & 2.9975 & -1 & 0 \\ 0 & 0 & 0 & -1 & 2.9975 & -1 \\ 0 & 0 & 0 & 0 & -1 & 2.9975 \end{bmatrix} \begin{bmatrix} U_{1,1} \\ U_{2,1} \\ U_{3,1} \\ U_{4,1} \\ U_{5,1} \\ U_{6,1} \end{bmatrix} = \begin{bmatrix} 2 \\ 0 \\ 0 \\ 0 \\ 0 \\ 0 \end{bmatrix}$$

M=0.2, we get

$$\begin{bmatrix} 2.95 & -1 & 0 & 0 & 0 & 0 \\ -1 & 2.95 & -1 & 0 & 0 & 0 \\ 0 & -1 & 2.95 & -1 & 0 & 0 \\ 0 & 0 & -1 & 2.95 & -1 & 0 \\ 0 & 0 & 0 & -1 & 2.95 & -1 \\ 0 & 0 & 0 & 0 & -1 & 2.95 \end{bmatrix} \begin{bmatrix} U_{1,1} \\ U_{2,1} \\ U_{3,1} \\ U_{4,1} \\ U_{5,1} \\ U_{6,1} \end{bmatrix} = \begin{bmatrix} 2 \\ 0 \\ 0 \\ 0 \\ 0 \\ 0 \end{bmatrix}$$

M=0.3, we get

$$\begin{bmatrix} 2.925 & -1 & 0 & 0 & 0 & 0 \\ -1 & 2.925 & -1 & 0 & 0 & 0 \\ 0 & -1 & 2.925 & -1 & 0 & 0 \\ 0 & 0 & -1 & 2.925 & -1 & 0 \\ 0 & 0 & 0 & -1 & 2.925 & -1 \\ 0 & 0 & 0 & 0 & -1 & 2.925 \end{bmatrix} \begin{bmatrix} U_{1,1} \\ U_{2,1} \\ U_{3,1} \\ U_{4,1} \\ U_{5,1} \\ U_{6,1} \end{bmatrix} = \begin{bmatrix} 2 \\ 0 \\ 0 \\ 0 \\ 0 \\ 0 \end{bmatrix}$$

These values of $U_{i,j}$ for $M=0.1, 0.2, 0.3, 0.4$ and 0.6 are presented in the table below.

Table 1; Values of $U_{i,j}$ for varying Magnetic field numbers at constant $Gr=2$

	M = 0.1	M = 0.2	M = 0.4	M = 0.6
H = 0.00	0.3823904	0.3907334	0.7999887	0.8195906
H = 0.01	0.1462153	0.1526635	0.3199673	0.3358333
H = 0.02	0.05588998	0.05962389	0.1279165	0.1375344
H = 0.03	0.0213149	0.0232270	0.05099042	0.05613971
H = 0.04	0.0080014	0.0088977	0.01995577	0.02246377
H = 0.05	0.002669	0.003015515	0.006881298	0.007882023

Graph of Velocity profiles against vertical plate height with varying magnetic field

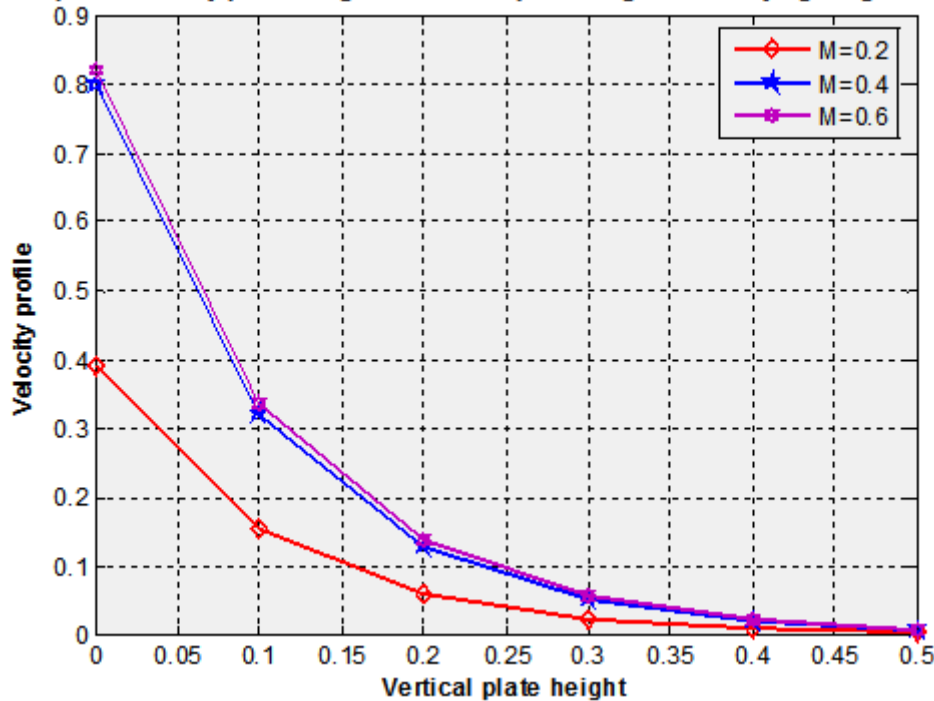


Figure 3: Graph of velocity against plate vertical height at varying magnetic field number

The figure depicts an increase of velocity profile for increasing magnetic field number, while it decreases along the plate. This is because the presence of a magnetic field introduces Lorentz force which slows down the motion of an electrically conducting fluid along the plate.

Taking $i=1, j=1, 2, 3, \dots$ our $y=i$ and $t=j$, $M=0.1$, $Gr=2$, and we get the matrix equation

$$\begin{bmatrix} 2.9975 & -1 & 0 & 0 & 0 & 0 \\ -1 & 2.9975 & -1 & 0 & 0 & 0 \\ 0 & -1 & 2.9975 & -1 & 0 & 0 \\ 0 & 0 & -1 & 2.9975 & -1 & 0 \\ 0 & 0 & 0 & -1 & 2.9975 & -1 \\ 0 & 0 & 0 & 0 & -1 & 2.9975 \end{bmatrix} \begin{bmatrix} U_{1,1} \\ U_{2,1} \\ U_{3,1} \\ U_{4,1} \\ U_{5,1} \\ U_{6,1} \end{bmatrix} = \begin{bmatrix} 2 \\ 0 \\ 0 \\ 0 \\ 0 \\ 0 \end{bmatrix}$$

Similarly if Grashof number is varied as Gr= 4 and 6, the values of $U_{i,j}$ are presented in the table below.

Table 2: Velocity(x, t) values for varying Grashof numbers at constant Magnetic field number M=0.1

	Gr = 2	Gr = 4	Gr = 6
H = 0.00	0.7647873	0.7814751	0.790609
H = 0.01	0.2924497	0.3053517	0.3125313
H = 0.02	0.1118309	0.1193124	0.123545
H = 0.03	0.04276337	0.04661974	0.048837779
H = 0.04	0.0163523	0.01821589	0.01930556
H = 0.05	0.00625266	0.007117133	0.007630975
H = 0.06	0.002390044	0.0022779651	0.003015041
H = 0.07	0.009114968	0.0010828337	0.00118802
H = 0.08	0.0003421678	0.0004147187	0.0004599166
H = 0.09	0.000114151	0.00014058	0.0001572365

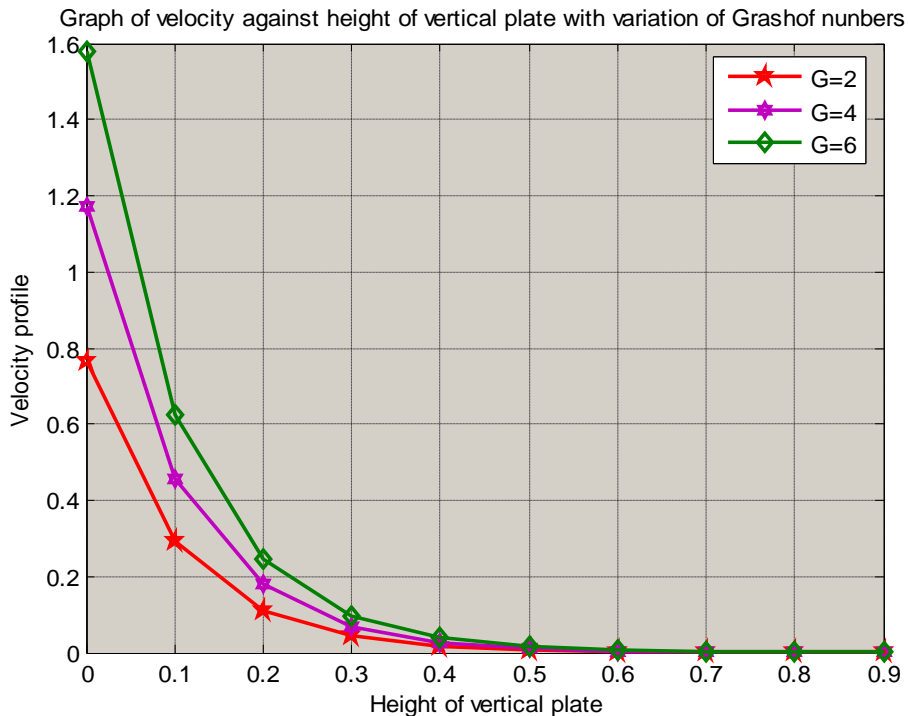


Figure 4: Graph of velocity against plate vertical height at varying Grashof numbers

Figure 4 shows an increase in velocity profile as the Grashof number increases at constant magnetic number and a decrease of velocity as the height of plate increases. This is because an increase in Grashof number has the tendency to increase the buoyancy effect which gives rise to an increase in the flow.

4.4.3 Energy Equation

The energy equation
$$\frac{\partial \theta}{\partial t} = \frac{1}{Pr} \frac{\partial^2 \theta}{\partial y^2} + \tau \left[\frac{\partial \theta}{\partial y} + Ec \left(\frac{\partial U}{\partial y} \right)^2 \right]$$
 (21)

We develop Implicit Crank Nicholson numerical scheme and discretize equation (21) as follows;

$$\frac{\theta_{i,j+1} - \theta_{i,j}}{\Delta t} = \frac{1}{Pr} \left[\frac{\theta_{i,j+1} - 2\theta_{i,j} + \theta_{i,j-1}}{(\Delta y)^2} \right] + Ec \left[\frac{U_{i,j+1} - U_{i,j}}{\Delta t} \right]^2$$
 (22)

Taking $i=1, j=0, 1, 2, 3, \dots$ our $y=i$ and $Ec=2, \tau=j$, and $Pr=0.71$

$$t \leq 0, U = 0, \theta = 0, y = 0$$

The equation (21) is solved subject to the boundary conditions

$$t > 0, U = 1, \theta = 1, \forall y \quad \text{for all } y$$

$$\Delta t = \Delta y = 0.05$$

We get the matrix equation

$$\begin{bmatrix} 2.035 & -1 & 0 & 0 & 0 & 0 \\ -1.035 & 2.035 & -1 & 0 & 0 & 0 \\ 0 & -1.035 & 2.035 & -1 & 0 & 0 \\ 0 & 0 & -1.035 & 2.035 & -1 & 0 \\ 0 & 0 & 0 & -1.035 & 2.035 & -1 \\ 0 & 0 & 0 & 0 & -1.035 & 2.035 \end{bmatrix} \begin{bmatrix} U_{1,1} \\ U_{2,1} \\ U_{3,1} \\ U_{4,1} \\ U_{5,1} \\ U_{6,1} \end{bmatrix} = \begin{bmatrix} 0.07 \\ 0 \\ 0 \\ 0 \\ 0 \\ 0 \end{bmatrix}$$

Table 3: Temperature, $\theta(x, t)$ values for varying Pr numbers at constant $Ec=2$

	Pr = 0.71	Pr = 0.5	Pr = 0.4	Pr = 0.2
H = 0.00	5.893902×10^{-2}	4.234904×10^{-2}	3.394071×10^{-2}	1.700106×10^{-2}
H = 0.01	4.994091×10^{-2}	3.554506×10^{-2}	2.856023×10^{-2}	1.434214×10^{-2}
H = 0.02	4.062786×10^{-2}	2.878272×10^{-2}	2.307214×10^{-2}	1.1760176×10^{-2}
H = 0.03	3.098885×10^{-2}	2.185133×10^{-2}	1.747429×10^{-2}	8.819835×10^{-3}
H = 0.04	2.101248×10^{-2}	1.474665×10^{-2}	1.176449×10^{-2}	5.909095×10^{-3}
H = 0.05	1.068694×10^{-2}	7.464353×10^{-3}	5.940483×10^{-3}	2.969924×10^{-3}

Graph of Temperature profiles against plate vertical height with varying Prandtl number

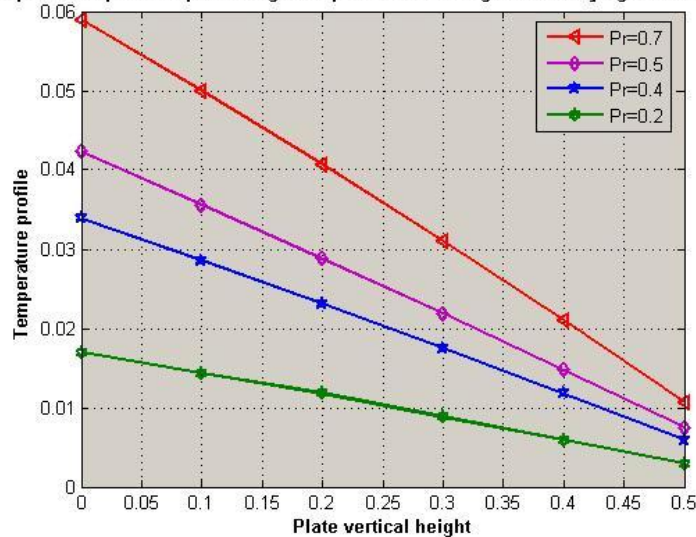


Figure 5: Graph of Temperature against plate vertical height at varying Prandtl numbers

From figure 5, it is evident that the temperature increases as the Prandtl number increases at constant Eckert number and a decrease in temperature as the plate height increases. Higher Prandtl number gives rise to increase heat transfer rates.

Table 4: Temperature, $\theta(x, t)$ values for varying Eckert numbers at constant Pr=0.2

	Ec = 4	Ec = 6	Ec = 8
H = 0.00	3.400212×10^{-2}	5.100318×10^{-2}	6.800424×10^{-2}
H = 0.01	2.868429×10^{-2}	4.302643×10^{-2}	5.736857×10^{-2}
H = 0.02	2.34035×10^{-2}	3.5105227×10^{-2}	4.680703×10^{-2}
H = 0.03	1.763967×10^{-2}	2.64595×10^{-3}	3.527934×10^{-2}
H = 0.04	1.181819×10^{-2}	1.772729×10^{-2}	2.363638×10^{-2}
H = 0.05	5.938493×10^{-3}	8.90774×10^{-3}	1.187699×10^{-2}

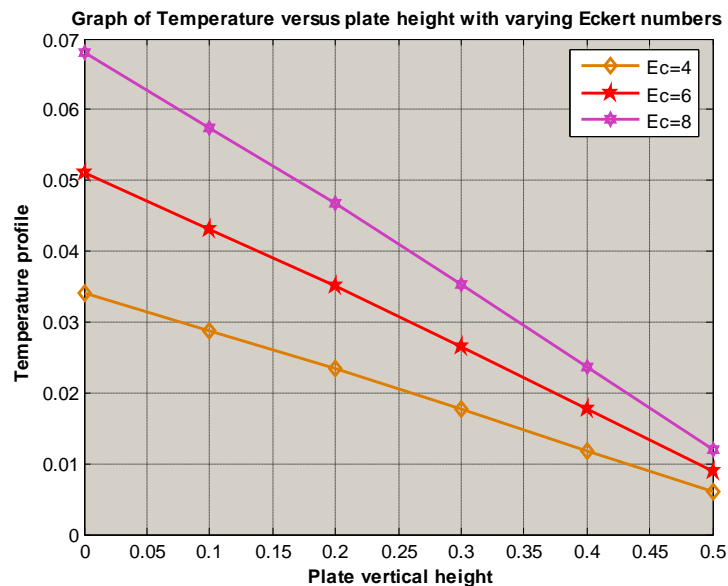


Figure 6: Graph of Temperature against plate vertical height at varying Eckert numbers

Figure 6 reveals a temperature increase with increase in Eckert number at constant Prandtl number while at the same time a decrease in temperature is evident as the height of the plate increases. Eckert number is the ratio of Kinetic energy of the flow to the boundary layer enthalpy difference that is viscous dissipation whose effect on the flow field is increased energy yielding greater fluid temperature.

V. Conclusion

A mathematical model has been presented for the steady two dimensional MHD free convective boundary layer flow of an electrically conducting Newtonian nanofluid over an impulsively started vertical plate. The governing boundary layer equations have been transformed into non-dimensional form and solved using the implicit finite difference method of Crank Nicolson type. It has been shown that the fluid velocity values increase across tables 1 and 2 with an increase in magnetic field and Grashof numbers as confirmed from figures 3 and 4 while temperature values increase with increase in Prandtl and Eckert numbers as shown in tables 3 and 4 as well as the graphs in figures 5 and 6. These results indicate that the magnetic field, Eckert, Prandtl and Grashof numbers have significant influences on velocity and temperature fields.

Further work is recommended to improve on the results so far obtained. This may be done by;

- (i) Considering the effect of other parameters such as the nano-particle volume fraction, Nusselt number and Buoyancy.
- (ii) Using another method of solution other than the FD method.

References

- [1]. Akharinia A, Abdolzadeh M, Laur R. (2011): critical investigation of heat transfer enhancement using nanofluids in micro-channels with slip and non-slip flow regimes. Journal of applications of thermal engineering **31**: 556-565.
- [2]. Aziz A, Khan WA (2012) Natural convective boundary layer flow of a nanofluid
- [3]. Boungiorno J. (2006) Convective transport in nanofluids. Journal of heat transfer **128**: 240-250.

- [4]. Capretto L, Cheng W, Hill M, Zhang X (2011): Micromixing within microfluidic devices. *Top Current Chemistry* **304**:27-68.
- [5]. Chamkhal A.J and Aly A.M (2011): MHD free convection flow of a nanofluid past a vertical plate in the presence of heat generation or absorption effects. *Chemical Engineering* **198**: 425-441.
- [6]. Choi S.U.S (2009): nanofluids: From vision to reality through research. *Journal of heat transfer* **131**: 1-9
- [7]. Ho C.H, Chen M.W, Li Z.W (2008): numerical simulation of natural convection of nanofluid in a square enclosure: effects due to uncertainties of viscosity and thermal conductivity. *International Journal of heat mass transfer* **47**: 4506-4516
- [8]. Keblinski P, Prasher R, Eapen J (2008): Thermal conductance of nanofluids. *Journal of Nanopart Res* **10**: 1089-1097.
- [9]. Khan W.A, Aziz A. (2011): Natural convection flow of a nanofluid over a vertical plate with uniform surface heat flux. *International Journal of Thermal Science* **50(7)**: 1207-1214.
- [10]. Kuznetsov A.V (2011): Non-oscillatory and oscillatory nanofluid bio-thermal convection in a horizontal layer of finite depth. *Euro Journal of Mec B/Fluids* **30**: 156-165.
- [11]. Matin M.H, Nohari M.R and Jahangiri P (2012): Entropy analysis in mixed convection MHD flow of nanofluid over a non-linear stretching sheet. *Journal of Thermal Science and Technology* **7**:1.
- [12]. Merkin J.H, Nazar R and Pop I (2012): The development of forced convection heat transfer near a forward stagnation point with Newtonian heating. *Journal of Engineering Math* **74**: 53-60.
- [13]. Narahari M, Dutta BK (2012) Effects of thermal radiation and mass diffusion on free convection flow near a vertical plate with Newtonian heating. *Chem Eng Comm* 199: 628–643.
- [14]. Niu J, Fu C, and Tan W (2012): Slip Flow and Heat Transfer of a non Newtonian Nanofluid in a Microtube. *PLoS ONE* **7(5)**: 37274.
- [15]. Nourazar S.S, Matin M, Hand Simiari M (2011): The HPM applied to MHD nanofluid flow over a horizontal stretching plate. *Journal of Applied Math*, **10**: 1155.
- [16]. past a convectively heated vertical plate. *Int J of Therm Sci* 52: 83–90.
- [17]. Yazdi M.H, Abdullah S, Hashim S and Sopian K (2011): slip MHD liquid flow and heat transfer over non-linear permeable stretching surface with chemical reaction. *International Journal of heat mass transfer* **54**: 3214-3225.
- [18]. Zeeshan A, Ellahil R, Siddiqui A.M, Rahman H.U (2012): An investigation of porosity and magnetohydrodynamic flow of non-Newtonian nanofluid in coaxial cylinders. *International Journal of Physical Science* **7(9)**: 1353-1361.